Preprints.org

Article

Influence of Magnetic Field on Atrazine Adsorption and Degradation by Ferroxite and Hematite

Marcos A. Sousa Antonio Sousa , Mateus Aquino Gonçalves [*] , Jessica Boreli dos Reis Lino , Stéfany Gonçalves de Moura , Joaquim Paulo da Silva , Teodorico Castro Ramalho

Article

Influence of Magnetic Field on Atrazine Adsorption and Degradation by Ferroxite and Hematite

Marcos A. Sousa [1], Mateus A. Gonçalves [1,*], Jéssica B. R. Lino [1], Stéfany G. Moura [1], Joaquim P. Silva [1] and Teodorico C. Ramalho [1,2,*]

[1] Laboratory of Molecular Modelling, Department of Chemistry, Federal University of Lavras, Lavras/MG, 37200-000 and Brazil

[2] Department of Chemistry, Faculty of Science, University of Hradec Kralove, Rokitanskeho 62, 500 03 Hradec Kralove, Czech Republic

* Correspondence: mateus.a.g@hotmail.com

Abstract: The study approaches the characterization of Ferroxite and Hematite and the test of their magnetic properties on the degradation and adsorption of Atrazine, an herbicide of the triazine class. This herbicide was compared with a sample of Ferroxite in the absence of magnetic field and with Hematite, a non-magnetic material which should not be attracted by the magnet. In the sample, the Atrazine determination was carried out by Fenton analysis. Preliminary results were satisfactory, gathering reduction rate up to 85% for Ferroxite in the presence of magnetic field and 53% for Hematite. The Fenton reaction, however, showed 87% reduction rate for Ferroxite in the presence of magnetic field, and 56% for Hematite. These findings have shown that there is a relation between the magnetic field intensity and the adsorption capacity for these materials.

Keywords: Fenton reaction; herbicide; magnetism

1. Introduction

The widespread use of agrochemicals is a significant concern in modern agriculture due to their potential to contaminate soil and water resources [1]. Studies have shown that common agrochemicals—including pesticides, fertilizers, hormones, and other growth-regulating agents—can lead to groundwater pollution through erosion and leaching processes [2,3]. Among these chemicals, Atrazine, a triazine-group herbicide, stands out as one of the most extensively used compounds. It is primarily applied to control broadleaf weeds in crops, both before and after their emergence (Figure 1).
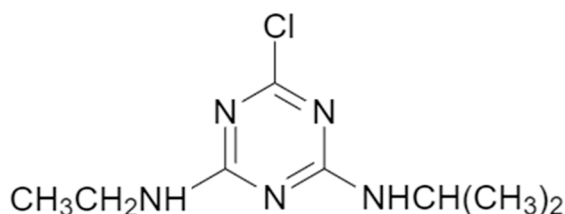

Figure 1. Chemical structure of Atrazine.

Atrazine is a widely used herbicide for controlling broadleaf and grassy weeds in crops such as sugarcane, sorghum, and corn [4]. Under low-temperature conditions, it remains stable and exhibits low adsorption potential, allowing for rapid mobility through the soil [5]. Since a significant portion of Atrazine is not absorbed by plants, it can disperse into the surrounding environment, posing a serious risk to human health. Due to its slow degradation rate and high potential for contaminating surface and groundwater, Atrazine is considered an environmental pollutant [6]. Adsorption onto activated carbon is one of the most commonly employed techniques for removing Atrazine from

water treatment systems, ensuring compliance with potable water standards [7]. Studies, such as those by Brito et al. [8], have shown that applying a magnetic field can significantly enhance the adsorption of environmental pollutants. However, Toledo et al. [9] highlight that this approach remains controversial due to its low reproducibility and inconsistent results. Despite these challenges, magnetic fields continue to be explored for water treatment applications. Additionally, factors such as magnetic impurities and dissolved oxygen levels present challenges in process control.

The adsorption of organic compounds and environmental pollutants under magnetic fields has been investigated by Singh, Ketan, and Singh [10], as well as by Yu, Zhou, and Jiang [11], who developed an efficient, recyclable magnetic titanium dioxide foam for enhanced pollutant removal. Ozeki et al. [12] also observed a correlation between magnetic field induction and the efficiency of adsorption and desorption processes. In this context, iron oxides can be combined with magnetic fields to improve pollutant removal. One such material is Ferroxite (δ-FeOOH), an iron oxyhydroxide characterized by the presence of O^{2-} and HO^- ions coordinated to the metal. Ferroxite possesses supermagnetic properties, high stability, and a large specific surface area [13], making it a promising candidate for Atrazine removal and degradation. First reported by Pereira et al. [14] as a photocatalyst in hydrogen production, Ferroxite exhibits a porous structure, high interparticle mesoporosity, small particle size, and a band-gap energy in the visible spectrum. These properties enhance the transfer and separation of photogenerated electrons and holes, improving its photocatalytic efficiency for Atrazine degradation. Tavares et al. [15] further explored the use of Ferroxite by studying the immobilization of soybean peroxidase and the removal of ferulic acid using free and immobilized enzymes.

Additionally, Ferroxite has been investigated in oxidative processes aimed at generating HO• radicals for Atrazine degradation, including hydrogen peroxide photolysis, Fenton processes, electrochemically assisted Fenton reactions [16,17], ozonation, and catalytic ozonation [18,19]. For comparative purposes, this study also examines Hematite, an antiferromagnetic iron oxide widely used for organic compound removal [20]. Hematite has demonstrated effectiveness in oxidative processes for the photocatalytic degradation of acetochlor, an herbicide used for weed control in agricultural fields [21]. Therefore, this study aims to evaluate the influence of magnetic fields on Atrazine adsorption and degradation using Ferroxite and Hematite.

2. Materials and Methods

2.1. Material

The material used in the study, as well as for the synthesis of Ferroxite, was as follows: sodium hydroxide at 5 mol.L-1 (Vertec Fine Chemicals of Brazil), hydrogen peroxide at 50%, ethanol, and ammoniacal ferrous sulfate (Vertec Fine Chemicals of Brazil). The Atrazine (Atrazine Atanor 50 SCAtanor of Brazil LTDA) was used for Atrazine curve construction, while the sodium chloride (Contemporary Chemical Dynamics LTDA), hydrochloric acid (QHEMIS), synthetic Ferroxite, ethanol and distilled water were used for the purpose of obtaining Zero Load Potential (ZLP).

The optimal mass of Ferroxite used in the trial to estimate values for Fenton analyses was obtained from a trial performed using different amounts of Ferroxite, Atrazine at 0.05 mg.L-1 concentration and different data collection times. For the estimation of values for Fenton analyses, the following trial conditions were used: Atrazine at 0.01 mg.L-1 and 0.2 mg.L-1 concentrations, 0.02 g and 0.05 g of Ferroxite, 0.02 g and 0.05 g of Hematite, and pH of 5 and 11. However, the following trial conditions were found to be appropriate for Fenton analyses: Atrazine at 0.01 mg.L-1, 0.05 g of Ferroxite, 0.05 g of Hematite, pH of 5 and different hydrogen peroxide volumes.

2.2. Synthesis of Ferroxite

The synthesis of Ferroxite (δ-FeOOH) followed the procedure described by Pereira et al. [14] and Pinto et al. [22]. This process involved a precipitation reaction in an alcoholic solution containing NaOH, leading to the formation of Fe^{2+} as a solid, followed by rapid oxidation with H_2O_2 to obtain the desired oxyhydroxide phase. Specifically, 31.36 g of ammoniacal ferrous sulfate (Vertec Fine Chemicals, Brazil) and 20 mL of 50% H_2O_2 were added to 200 mL of deionized water under constant

stirring at 60°C for 30 minutes to promote oxidation. Subsequently, 100 mL of 5 mol.L^{-1} NaOH solution (Vertec Fine Chemicals, Brazil) was introduced to induce precipitation.

The resulting precipitate was thoroughly washed with distilled water to remove residual ions and then rinsed with ethanol to facilitate drying and prevent aggregation. Finally, the material was dried in an oven at 60°C for 24 hours to ensure complete removal of solvent residues and stabilization of the Ferroxite structure. The synthesized material was then characterized to confirm its phase purity, morphology, and physicochemical

2.3. Standard Atrazine Curve for Analyses of Fenton

After the synthesis and characterization of Ferroxite, Fenton degradation experiments were planned to evaluate its catalytic activity. To monitor the efficiency of the process, a standard Atrazine curve was constructed based on the Lambert-Beer law, allowing the estimation of minimum and maximum values for further tests. Atrazine standards were prepared at the following concentrations: 0.010, 0.025, 0.050, 0.100, 0.200, and 0.250 mg.L^{-1} and analyzed in a UV-VIS spectrophotometer. Table S1 (Online Resource) describes the absorbance values for each concentration shown in the Atrazine curve (Figure 2).
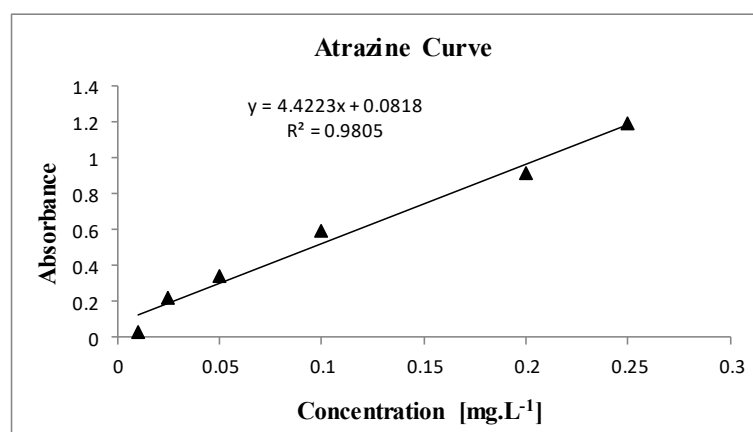

Atrazine Curve

$y = 4.4223x + 0.0818$
$R^2 = 0.9805$

Figure 2. Absorbance obtained as function of Atrazine concentration.

2.4. Obtaining of the Zero Load Potential

The Zero Load Potential (ZLP) corresponds to the pH at which the adsorbent surface has an overall neutral charge, or alternatively, the pH at which the maximum hydrogen production rate from water occurs. When the solution pH is lower than the ZLP of the material under study, the adsorbent surface becomes positively charged. Conversely, when the solution pH is higher than the ZLP, the adsorbent surface becomes negatively charged [22]. The methodology used to determine the ZLP is the "11-point experiment" [23], which typically employs pH values ranging from 1 to 12. However, in this study, 12 points were used, with pH values ranging from 2 to 13, aiming for higher accuracy in the measurements. The pH values were adjusted from 2 to 13 by adding 0.1 mol.L^{-1} HCl or 0.1 mol.L^{-1} NaOH to a 30 mL solution of 0.01 mol.L^{-1} NaCl. Then, 0.015 g of Ferroxite was added to each 10 mL of pH-adjusted solution and kept under constant stirring for 48 hours. After this period, the final pH values were measured to construct the ZLP curve as a function of pH. Table S2 (Online Resource) presents the results obtained, and Figure 2 illustrates the ZLP curve.

2.5. Mass of Ferroxite

The experiment was conducted to determine the optimal Ferroxite mass range for adsorption and degradation studies, based on absorbance reduction measurements. By evaluating different mass values, it was possible to identify conditions that maximize the removal efficiency of Atrazine while maintaining experimental feasibility. To achieve this, different amounts of Ferroxite (0.01, 0.02, 0.03, 0.04, and 0.05 g) were added to separate samples, each containing 20 mL of 0.05 mg.L^{-1} Atrazine

solution. The samples were then subjected to a controlled magnetic field for 0, 1, and 2 hours, allowing the evaluation of possible interactions between Ferroxite and the pollutant under different conditions. After the exposure period, the absorbance of each sample was measured using a UV-VIS spectrophotometer, providing insights into the material's efficiency in degrading or adsorbing Atrazine over time. The results obtained from this experiment are summarized in Table S3 (Online Resource), which presents the Ferroxite mass values tested and their corresponding effects on absorbance reduction. These findings were essential for defining the experimental parameters used in subsequent adsorption and photocatalysis tests.

2.6. Determination of Values for Fenton Analyses by Means of Removal by Adsorption

The values used in this study were based on the minimum and maximum estimates obtained for each parameter under investigation: (i) 0.010 mg·L^{-1} and 0.2 mg·L^{-1} in the Atrazine curve according to the Lambert-Beer law for spectrophotometry; (ii) 0.02 g and 0.05 g of Ferroxite, which allowed the measurement of lower and higher adsorption, respectively; (iii) Hematite, an antiferromagnetic mineral used in this study for comparative purposes; and (iv) pH values selected to determine the minimum and maximum estimates on the ZLP curve.

Estimates of 0.02 g and 0.05 g of Ferroxite and Hematite were added each to samples comprising 20 mL of Atrazine at 0.01 mg.L-1 and 0.20 mg.L-1 concentration, and pH values ranging from 5 to 11 (Table 1 and Table 2). The absorbance was measured after 0, 1 and 2 hours, then to estimate the removal percentage by adsorption, using the following equation.

$$\text{Reduction rate [\%]} = \frac{(\text{Absorbance}_{initial} - \text{Absorbance}_{measured})}{\text{Absorbance}_{initial}} x100$$

Table 1 shows values of adsorption percentage for Ferroxite and Table 2 shows values of adsorption percentage for Hematite, both in the presence and absence of magnetic field.

Table 1. Values of adsorption percentage for Ferroxite used for the determination of values for analyses by means of removal by adsorption, in the presence and absence of magnetic field.

Experimental Conditions A = Atrazine [mg.L^{-1}] F =Ferroxite [g]	Adsorption Percentage (%)	
	Sample in the absence of magnetic field	Sample in the presence of magnetic field
1. A(0.01)/F(0.02)/pH(5)/1h	39.64	56.52
2. A(0.01)/F(0.02)/pH(5)/2h	63.03	5.95
3. A(0.01)/F(0.02)/pH(11)/1h	33.83	76.70
4. A(0.01)/F(0.02)/pH(11)/2h	33.56	76.82
5. A(0.01)/F(0.05)/pH(5)/1h	73.17	85.88
6. A(0.01)/F(0.05)/pH(5)/2h	81.05	77.10
7. A(0.01)/F(0.05)/pH(11)/1h	29.85	63.77
8. A(0.01)/F(0.05)/pH(11)/2h	50.39	0.00
9. A(0.2)/F(0.02)/pH(5)/1h	1.88	1.88
10. A(0.2)/F(0.02)/pH(5)/2h	3.25	3.25
11. A(0.2)/F(0.02)/pH(11)/1h	39.31	33.95
12. A(0.2)/F(0.02)/pH(11)/2h	39.31	43.06
13. A(0.2)/F(0.05)/pH(5)/1h	25.82	2.80
14. A(0.2)/F(0.05)/pH(5)/2h	52.69	2.85
15. A(0.2)/F(0.05)/pH(11)/1h	0.00	20.56
16. A(0.2)/F(0.05)/pH(11)/2h	0.00	4.98

Table 2. Values of adsorption percentage for Hematite used for the determination of values for analyses by means of removal by adsorption, in the presence and absence of magnetic field.

Experimental Conditions A = Atrazine [mg.L⁻¹] H =Hematite [g]	Adsorption Percentage (%)	
	Sample in the absence of magnetic field	Sample in the presence of magnetic field
1. A(0.01)/H(0.02)/pH(5)/1h	19.24	31.34
2. A(0.01)/H(0.02)/pH(5)/2h	28.99	51.78
3. A(0.01)/H(0.02)/pH(11)/1h	29.23	0.00
4. A(0.01)/H(0.02)/pH(11)/2h	8.85	37.78
5. A(0.01)/H(0.05)/pH(5)/1h	10.96	53.49
6. A(0.01)/H(0.05)/pH(5)/2h	29.08	65.75
7. A(0.01)/H(0.05)/pH(11)/1h	53.18	29.67
8. A(0.01)/H(0.05)/pH(11)/2h	44.54	26.18
9. A(0.2)/H(0.02)/pH(5)/1h	18.06	25.90
10. A(0.2)/H(0.02)/pH(5)/2h	30.78	33.25
11. A(0.2)/H(0.02)/pH(11)/1h	0.00	10.28
12. A(0.2)/H(0.02)/pH(11)/2h	12.41	15.60
13. A(0.2)/H(0.05)/pH(5)/1h	26.07	45.87
14. A(0.2)/H(0.05)/pH(5)/2h	36.00	54.78
15. A(0.2)/H(0.05)/pH(11)/1h	9.23	0.53
16. A(0.2)/H(0.05)/pH(11)/2h	18.69	28.97

3. Results

3.1. Evaluation of Experimental Conditions

Building upon the methodology outlined previously, the following results were obtained: an R-squared (R^2) value of 0.9805 was achieved for the Standard Atrazine Curve (Figure 2), in line with the Lambert-Beer law. Atrazine concentrations ranging from 0.010 to 0.250 mg·L⁻¹ were employed to derive the minimum and maximum estimates required for the adsorption and degradation processes.

The results obtained in this study are consistent with expectations based on the Lambert-Beer law, as indicated by the high R-squared (R^2) value of 0.9805 for the Standard Atrazine Curve (Figure 2). This strong correlation suggests that the absorbance measurements reliably correspond to Atrazine concentrations within the range tested, reinforcing the accuracy of the spectrophotometric method used. The concentration range of 0.010 to 0.250 mg·L⁻¹ was effective in capturing the variability needed to evaluate both the adsorption and degradation processes. These concentrations allowed for a clear distinction between the minimum and maximum estimates of Atrazine, providing valuable insight into the efficiency of the processes under study. Furthermore, the ability to accurately measure these concentrations under varying experimental conditions supports the robustness of the experimental design and the potential for further exploration into the factors influencing Atrazine removal.

In addition, pH is a critical parameter related to adsorption, as it influences the physical and chemical characteristics of the adsorbent surface, which in turn affects the estimation of the zeta potential (ZLP). The ZLP allows for the estimation of the charge on the adsorbent surface as a function of pH values. This parameter indicates whether the adsorbent surface is neutral, positive, or negative, depending on the pH of the solution. Figure 3 illustrates the ZLP curve obtained as a function of pH, and Table S2 (Online Resource) provides the initial and final pH values, as well as the difference between them.

Additionally, trials were conducted to determine the optimal mass of Ferroxite, and the minimum and maximum estimates for Atrazine removal by adsorption were selected. These estimates were based on the observed performance across varying conditions, providing valuable insights into the efficiency of the adsorption process. Table S3 presents the results corresponding to these estimates, highlighting the impact of Ferroxite mass on the removal efficiency of Atrazine.
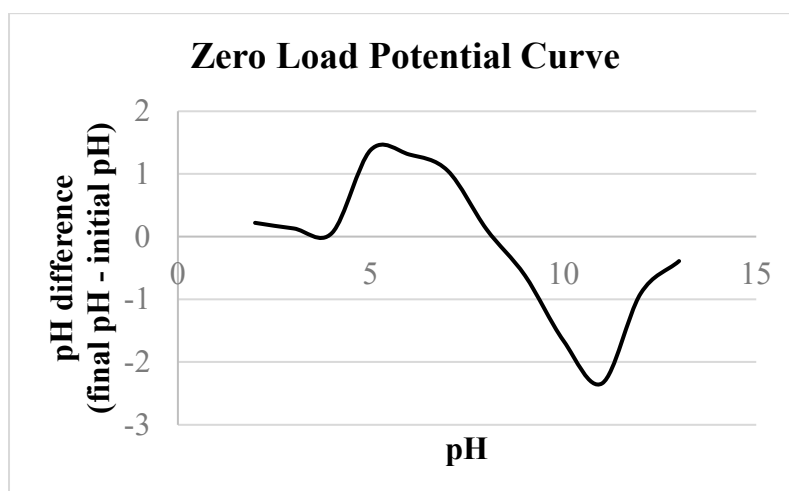
Figure 3. ZLP curve got as function of pH.

3.1. Evaluation of Experimental Conditions

To complement the discussion, it is important to note the impact of the magnetic field on the adsorption process for both Ferroxite and Atrazine. The increase in removal percentage from 81.05% to 85.88% in the presence of a magnetic field suggests that the application of the magnetic field may enhance the interaction between Ferroxite and Atrazine, possibly by promoting better dispersion of the adsorbent or altering the surface properties of Ferroxite, thereby increasing its efficiency in adsorbing Atrazine.

Moreover, while the removal percentage for Ferroxite adsorption in the absence of a magnetic field after 1 hour was 73.16%, this highlights the role of time in the adsorption process. The data suggests that, in the absence of a magnetic field, the equilibrium adsorption may not be fully reached within the first hour, and further experimentation over extended time periods could be necessary to optimize the adsorption process. This could also provide insights into the kinetics of the adsorption process, helping to determine the ideal equilibrium time for maximum Atrazine removal. Further studies could explore the influence of various factors, such as the concentration of Atrazine, the weight of Ferroxite, and the pH, on the overall performance of the adsorption process. Additionally, investigating the long-term stability of the magnetic field's effect and comparing it with other adsorbents or methods could be beneficial in optimizing treatment systems for Atrazine removal in environmental applications.

To complement this discussion, it is important to highlight the inherent differences in the magnetic properties of Hematite and Ferroxite, which directly influence their adsorption performance. The lower removal percentage for Hematite (53.18%) compared to Ferroxite (73.16%) in the absence of a magnetic field suggests that Hematite's weak magnetic remanence and antiferromagnetic behavior limit its efficiency in adsorbing Atrazine. The negative exchange interactions between subsequent basal planes and the opposing magnetic moments in Hematite may hinder the material's ability to interact effectively with Atrazine, resulting in lower adsorption capacity.

However, when a magnetic field is applied, the removal by adsorption for both materials increased, but the effect was much more pronounced for Ferroxite, with a rise from 73.16% to 85.88%. In contrast, Hematite showed only a slight increase in removal (53.18% to 53.49%). This sharp contrast further demonstrates that the magnetic field has a much more significant influence on Ferroxite, possibly by aligning its magnetic moments and enhancing its interaction with Atrazine molecules. The external magnetic field likely helps to increase the dispersion of Ferroxite particles, facilitating better adsorption. In contrast, Hematite's minimal response to the magnetic field, with only a slight increase in removal, supports the hypothesis that its antiferromagnetic properties prevent the field from significantly altering its behavior, limiting the enhancement of adsorption. Therefore, the findings suggest that Ferroxite, with its stronger magnetic properties, is better suited for Atrazine

removal in the presence of a magnetic field, whereas Hematite's adsorption performance is largely unaffected by the application of a magnetic field due to its inherent antiferromagnetic characteristics.

3.1. Evaluation of Experimental Conditions

The concentration of hydrogen peroxide was assessed aiming at optimizing degradation conditions using the best procedures described for optimization of adsorption conditions. The following parameters were used: x-axis for Atrazine concentration (mg.L-1), y-axis for Ferroxite mass (g), pH, and the reaction time. Greater values on degradation were found after 1 hour, in the presence of magnetic field (Table 1, trial #5 for Ferroxite and Table 2, trial #5 for Hematite). Trial conditions were the same for Ferroxite and Hematite, as follows: 0.01 mg.L-1 of Atrazine, 0.05 g of the mineral, and pH at 5 in the presence of magnetic field. However, Fenton reactions were carried out in the absence of magnetic field for comparative purpose.

The greater value on removal by degradation for Ferroxite was 64.49%, with hydrogen peroxide consumption at 1.1 mL, in the absence of magnetic field (Table 3, trial #6). However, in the presence of magnetic field, the removal by degradation for Ferroxite was 87.53%, with hydrogen peroxide consumption at 0.9 mL (Table 3, trial #5), showing the influence of magnetic field on Atrazine degradation by Ferroxite.

Table 3. Degradation percentage of Atrazine by Ferroxite in the presence and absence of magnetic field, at different hydrogen peroxide consumption.

Experimental Conditions H_2O_2 [mL]	Degradation Percentage (%)	
	Sample in the absence of magnetic field	Sample in the presence of magnetic field
1. H_2O_2(0.1)/1h	3.12	0.00
2. H_2O_2(0.3)/1h	21.95	0.00
3. H_2O_2(0.5)/1h	36.43	14.41
4. H_2O_2(0.7)/1h	19.18	80.34
5. H_2O_2(0.9)/1h	46.42	87.53
6. H_2O_2(1.1)/1h	64.49	73.88
7. H_2O_2(1.3)/1h	58.03	48.53
8. H_2O_2(1.5)/1h	30.83	64.40

The highest removal by degradation for Hematite was 28.82% in the absence of a magnetic field, with hydrogen peroxide consumption of 0.7 mL (Table 4, trial #4). However, when exposed to a magnetic field, the degradation efficiency for Hematite showed a marked improvement, reaching 56.35%, with a corresponding reduction in hydrogen peroxide consumption to 0.5 mL (Table 4, trial #3). These findings underscore the significant influence of the magnetic field on the catalytic activity of Hematite, highlighting its role in enhancing the degradation of Atrazine. The magnetic field appears to facilitate the generation of reactive species or promote a more efficient interaction between the Hematite surface and hydrogen peroxide, thereby increasing the mineral's effectiveness in the degradation process. This enhancement demonstrates the potential for optimizing Hematite-based systems in environmental applications, where the combination of magnetic properties and catalytic activity could lead to more efficient and sustainable remediation strategies for Atrazine and other pollutants.

Table 4. Degradation percentage of Atrazine by Hematite in the presence and absence of magnetic field, at different hydrogen peroxide consumption.

Experimental Conditions H_2O_2 [mL]	Degradation Percentage (%)	
	Sample in the absence of magnetic field	Sample in the presence of magnetic field
1. H_2O_2(0.1)/1h	3.33	0.00

2. $H_2O_2(0.3)/1h$	0.00	0.00
3. $H_2O_2(0.5)/1h$	18.34	56.35
4. $H_2O_2(0.7)/1h$	28.82	3.90
5. $H_2O_2(0.9)/1h$	25.60	24.11
6. $H_2O_2(1.1)/1h$	23.53	15.17
7. $H_2O_2(1.3)/1h$	12.66	13.34

The values for removal by degradation were notably higher in the presence of a magnetic field, emphasizing the significant influence of the magnetic field on the degradation process. Moreover, the removal efficiency for Ferroxite was consistently superior to that observed for Hematite, underscoring the dual impact of both the magnetic field and the mineral type on Atrazine adsorption and degradation. These results highlight Ferroxite's greater effectiveness in the degradation process, likely due to its ability to generate free radicals during Fenton reactions, leading to a remarkable 87% removal of the Atrazine organic charge. In addition to its enhanced catalytic activity, the magnetic properties of Ferroxite offer an additional advantage, facilitating its easy recovery and potential reuse in other heterogeneous processes, thus making it an attractive candidate for sustainable and efficient water treatment applications.

5. Conclusions

The present study showed that the removal values by adsorption for Ferroxite were significantly higher in the presence of a magnetic field compared to those observed in its absence, demonstrating the clear influence of the magnetic field on Atrazine degradation by Ferroxite. This magnetic effect was more pronounced for Ferroxite than for Hematite, which exhibited antiferromagnetic behavior, further highlighting the role of magnetic properties in the adsorption process. The Fenton process was used to assess the reactivity of Atrazine with both Ferroxite and Hematite under specific hydrogen peroxide consumption conditions. The results indicated that the Fenton process was more efficient for Ferroxite in the presence of the magnetic field, outperforming both Ferroxite in the absence of the magnetic field and Hematite in both conditions. These findings emphasize the positive impact of the magnetic field on the interaction between Ferroxite and Atrazine, suggesting that Ferroxite, when exposed to a magnetic field, offers superior efficiency in Atrazine degradation, highlighting its potential for more effective environmental remediation strategies.

Supplementary Materials: The following supporting information can be downloaded at the website of this paper posted on Preprints.org.

References

1. Bailey, G.W.; White, J.L. Single Pesticide Volume: The Triazine Herbicides. In Pesticide Chemistry: The Model of the Triazine Herbicides, Gunther, F.A., Gunther, J.D., Eds.; Springer Verlag: New York, 1970; Volume 32, pp. 29–92. https://doi.org/10.1007/978-1-4615-8464-3_4

2. Brigante, J.; et al. Environmental Evaluation of the Mogi-Guaçu River: Results of a Research with an Ecosystem Approach. Rima: São Carlos, 2002, p. 58.

3. Veiga, M.M.; et al. Cad. Saúde Pública 2006, 22, 1–9. https://doi.org/10.1590/S0102-311X2006001100013

4. Mehler, W.T.; Schuler, L.J.; Lydy, M.J. Environmental Pollution 2008, 153, 331–337. https://doi.org/10.1016/j.envpol.2007.04.028

5. Egler, M. Utilizing the Benthonic Macroinvertebrate Community of Evaluation of Degradation of Rivers Ecosystems in Agricultural Areas. Dissertation, Oswaldo Cruz Foundation: Rio de Janeiro, 2002; p. 147.

6. Graymore, M.; Stagnitti, F.; Allinson, G. Environ. Int. 2001, 27, 243–248. https://doi.org/10.1016/S0160-4120(01)00031-9

7. Jiang, H.; Adams, C. Water Research 2006, 40, 527–532. https://doi.org/10.1016/j.watres.2006.02.013

8. Brito, J.F.; et al. Water, Air, Soil Pollut. 2012, 223, 2195–2203. https://doi.org/10.1007/s11270-012-1132-6

9. Toledo, E.J.; et al. J. Mol. Struct.: THEOCHEM 2009, 902, 62–67. https://doi.org/10.1016/j.theochem.2009.08.035

10. Singh, A.K.; Ketan, K.; Singh, J.K. Environ. Chem. Eng. 2017, 5, 507–514. https://doi.org/10.1016/j.jece.2017.09.060

11. Yu, L.; Zhou, X.; Jiang, W. Ind. Eng. Chem. Res. 2016, 55, 5394–5401. https://doi.org/10.1021/acs.iecr.6b02278

12. Ozeki, S.; et al. J. Phys. Chem. 1996, 100, 11843–11847. https://doi.org/10.1021/jp9528774

13. Chagas, P.; et al. J. Nanopart. Res. 2013, 15, 1747–1756. https://doi.org/10.1007/s11051-013-1544-2

14. Pereira, M.C.; et al. J. Mater. Chem. 2011, 21, 13085–13094. https://doi.org/10.1039/C1JM11736J

15. Tavares, T.S.; et al. Bioprocess Biosyst. Eng. 2018, 41, 1281–1291. https://doi.org/10.1007/s00449-017-1848-1

16. Laat, J.; et al. Chemosphere 1999, 39, 1577–1588. https://doi.org/10.1016/S0045-6535(99)00204-0

17. Ventura, A.; et al. J. Adv. Oxid. Technol. 2002, 5, 90–95. https://doi.org/10.1515/jaots-2002-0114

18. Acero, J.L.; Stemmler, K.; Von Gunten, U. Environ. Sci. Technol. 2000, 34, 4810–4816. https://doi.org/10.1021/es990724e

19. Ma, J.; Graham, N.J.D. Water Research 2000, 34, 4754–4762. https://doi.org/10.1016/S0043-1354(00)00130-5

20. Siqueira, D.S.; Marquer Jr., J.; Pereira, G.T. Geoderma 2010, 155, 109–115. https://doi.org/10.1016/j.geoderma.2009.11.024

21. Fu, Y.; et al. Optik 2019, 183, 513–519. https://doi.org/10.1016/j.ijleo.2018.10.018

22. Pinto, I.S.X.; et al. Appl. Catal., B 2012, 118, 131–141. https://doi.org/10.1016/j.apcatb.2012.02.026

23. Robles, J.; Regalbuto, J.R. The Engineering of Pt/Carbon Catalyst Preparation: for Application on Proton Exchange Fuel Cell Membrane (PEFCM); University of Illinois: Chicago, 2004; p. 14.

24. Silva, F.M.; et al. Cadernos de Pesquisa 2010, 17, 3, 67–82.